



1 Predictive Performances of Machine Learning– and Deep Learning–Based Univariate and Multivariate 2 Reservoir Inflow Predictions in the Chao Phraya River Basin

3
4 Jidapa Kraisangka^a, Pheeranat Dornpunya^{b, c}, Areeya Rittima^{b*}, Wudhichart Sawangphol^a, Yutthana Phankamolsil^d, Allan Sriratana Tabucanon^c,
5 Yutthana Talaluxmana^f, and Varawoot Vudhivanich^g

6
7 ^a Faculty of Information and Communication Technology, Mahidol University, Thailand
8
9 ^{b, b*} Graduate Program in Environmental and Water Resources Engineering, Department of Civil and Environmental Engineering, Faculty of Engineering,
10 Mahidol University, Thailand
11
12 ^c Hydro-Informatics Institute (Public Organization), Thailand
13
14 ^d Environmental Engineering and Disaster Management Program, Mahidol University, Kanchanaburi Campus, Thailand
15 ^e Faculty of Environment and Resource Studies, Mahidol University, Phutthamonthon, Nakhon Pathom, Thailand
16 ^f Department of Water Resources Engineering, Faculty of Engineering, Kasetsart University, Thailand
17 ^g Department of Irrigation Engineering, Faculty of Engineering at Kamphaeng Saen, Kasetsart University, Thailand

18 *Corresponding author(s). E-mail(s): areeya.rit@mahidol.ac.th; Contributing authors: jidapa.kra@mahidol.ac.th; pheeranat.dor@gmail.com;
19 wudhichart.saw@mahidol.ac.th; yutthana.pha@mahidol.ac.th; allansriratana.tab@mahidol.ac.th; fengyt@ku.ac.th; fengvvw@ku.ac.th

20 Abstract

21 This study demonstrated the predictability of Machine Learning (ML)– and Deep Learning (DL)–based univariate and
22 multivariate predictions of reservoir inflows of Bhumibol (BB) and Sirikit (SK), two major dams in the Chao Phraya
23 River Basin. XGBoost, tree–based ensemble–, and LSTM, deep neural network–based algorithms were selected for
24 development of daily and monthly prediction models. For univariate prediction, the inflows of the BB and SK dams
25 were predicted separately using two individual models. In contrast, for multivariate prediction, a single model was
26 developed to simultaneously predict the inflows of both the BB and SK dams facilitating the integrated decision–
27 making processes. Across all prediction scenarios, ML– and DL–based models demonstrated superior performances
28 in predicting daily reservoir inflows for BB and SK dams compared to monthly predictions, achieving NSE values of
29 0.86 and 0.77, respectively. Since modeling with LSTM algorithm can effectively handle larger datasets, this enables
30 single multivariate prediction model to predict closer results to those individual univariate models performed by
31 XGBoost and LSTM for BB and SK prediction. XGBoost models mostly outperformed LSTM when tested on the
32 datasets for both daily and monthly univariate predictions. Among all prediction scenarios, underprediction of low
33 reservoir inflows and overprediction of high reservoir inflows by both univariate and multivariate models were
34 consistently existed. Therefore, extracting specific and informative insights from the results of each model type,
35 forecasting horizon, and algorithms used can significantly enhance decision–making support for both real–time
36 reservoir operation and long–term reservoir management planning.

37 **Keywords:** Machine Learning (ML), Deep Learning (DL), Artificial Intelligence (AI), Reservoir Inflow Prediction,
38 Chao Phraya River Basin

39 1. Introduction

40 The increased climate variability has intensified the water–related challenges globally making the water
41 resources management more complicated under the changing circumstances (Ngamsanroaj and Tamee, 2019).
42 Consequently, risks of water stress and scarcity exacerbated by reservoir operation and management have substantially
43 increased. A key factor contributing to this is uncertain water supply in the reservoir system. Reservoir inflow is
44 commonly considered as the principal source of water supply in reservoirs. It is significantly influenced by the climate
45 variability and hydrologic phenomena. Accurate and precise reservoir inflow prediction plays a crucial role for
46 effective reservoir planning and management (Suprayogi et al., 2020). During critical climate events, future reservoir
47 inflow forecast informs decision making for instant operational responses to natural disasters like floods and drought.
48 During normal climate conditions, predictive reservoir data is used for establishment of guideline trajectory for proper
49 reservoir operation. Predicting the precise reservoir inflow is inherently stochastic due to uncertainty of hydrological
50 inputs and strong non–linearity of the system (Soncin et al., 2024). For decades, numerous research studies have been
51 dedicated to reservoir inflow predictions to achieve the desired purposes for both reservoir management planning and
52 real–time operation.

53 A wide range of prediction techniques including physically process–based–, conventional stochastic–based–
54 and modern data–driven approaches like Machine Learning (ML) and hybrid models have been widely employed to
55 enhance the model predictability. It is revealed that the process–based hydrological models usually rely on a various
56 number of assumptions and require many physical parameters to resemble the hydrological nature of environment
57 (Firat and Güngör, 2008; Luo et al., 2020). In addition, the conventional stochastic–based techniques such as ARMA,
58 ARIMA for time series prediction provided good results for only linear data. However, it is not appropriate for non–



60 linearity phenomenon influenced by climate, natural geography, and human activities (Valipour et al., 2013).
61 Prediction time horizon selected has been generally ranged from short-term (hourly, daily, weekly) to long-term
62 predictions (monthly, seasonal, yearly). Univariate prediction model is generally used to predict future values of single
63 variable using the historical data. While, multivariate prediction model involves predicting the future values of
64 multiple interrelated variables. However, short-term univariate prediction predicting future values of single reservoir
65 inflow has broadly been found particularly for real-time operation and short-term planning. Predicting multiple
66 reservoir inflows using multivariate prediction model by taking the interdependencies of influencing factors of
67 multiple reservoirs has rarely studied and limited.

68 The advancement of Artificial Intelligence (AI) and Machine Learning (ML) approach has revolutionized
69 transformative impacts across the traditional prediction methods and their disciplines. A great deal of data-driven ML
70 approach has enhanced the predictability for hydrological prediction (Zhang et al., 2018) such as rainfall (Chen et al.,
71 2017; Ridwan et al., 2021), streamflow (Latif et al., 2023; Kisi et al., 2024), reservoir inflow (Zhang et al., 2021;
72 Hameed et al., 2022; Latif et al., 2024), reservoir water level (Sapitang et al., 2020; Aquil and Ishak, 2023), river water
73 level (Ahmed et al., 2023; Zakaria et al., 2023), groundwater level (Osman et al., 2020), sediment transport
74 (Almubaidin et al., 2023), water quality prediction (Haghiabi et al., 2018; Shams et al., 2024) and snow water
75 equivalent (Khosravi et al., 2023).

76 Since 1990s, a well-known Artificial Neural Networks (ANNs) inspired by human brain structure and its
77 function has intensively been used for hydrological prediction. It was commonly applied for both univariate and
78 multivariate predictions. For example, univariate time series prediction of reservoir inflow was developed using ANNs
79 to map the non-linear relationships between input and output variables (Kawade et al., 2019). Many studies also
80 revealed that ANNs significantly outperformed than the statistically-stochastic-based prediction models like AR, MA,
81 and ARIMA for the reservoir inflow prediction (Pradeepakumari and Srinivasu, 2019). Additionally, ANNs can be
82 applicable for both parametric and non-parameter data (Pini et al., 2020).

83 The rapid evolution of ML algorithms has been driven by the advancement and succession of computer
84 science and technologies to increase the computational capability and handle large dataset. Consequently, the
85 improved ML algorithms have been progressively developed incorporating supervised learning, unsupervised
86 learning, and reinforcement learning for various tasks. Several conventional ML algorithms have commonly been
87 employed for reservoir inflow prediction such as Support Vector Machines (SVM), K-Nearest Neighbors (KNN),
88 Random Forest (RF), Multi-layer Perceptron (MLP), Gradient Boosting (GB), Extreme Gradient Boosting
89 (XGBoost), and Radial Bias Function (RBF). A comparative study for daily reservoir inflow prediction was conducted
90 using four different approaches; (1) Multiple Linear Regression (MLR), (2) Random Forest (RF), (3) Extreme
91 Learning Machine (ELM), and (4) Regularized Extreme Learning Machine (RELM). The results showed the
92 superiority of RELM approach that yielded higher prediction accuracy with $R = 0.955$ (Hameed et al., 2022).
93 XGBoost, a relatively recent algorithm, has proven its effectiveness in reservoir inflow prediction. To forecast multi-
94 step ahead daily and monthly reservoir inflows, XGBoost was ranked as the best prediction model compared to MLP,
95 Support Vector Regression (SVR), Adaptive Neuro-Fuzzy Inference System (ANFIS) (Ibrahim et al., 2023). Similarly,
96 XGBoost outperformed RF and an ensemble model combining XGBoost-RF algorithms for daily reservoir inflow
97 prediction (Jan et al., 2024)

98 Recently, achievement of Deep Learning (DL) which is a subset of ML, has renowned incorporating multiple
99 layers artificial neural networks or Deep Neural Networks (DNNs) with automatic feature learning. It is indicated that
100 DL is powerful in extracting complex features hidden in vast amount of hydrological dataset (Huang et al., 2022).
101 Some of the most widely used DL algorithms for time series prediction are Convolutional Neural Networks (CNNs),
102 Recurrent Neural Networks (RNNs), Long-Short Term Memory (LSTM), and Gated Recurrent Unit (GRU). GRU is
103 the simplified form of LSTM well-suited for faster training for time series prediction. While, LSTM is a specific type
104 of RNNs designed to learn the long-term temporal dependency and seasonality of time series data and overcome the
105 vanishing and exploding gradient problems of RNNs (Dtissibe et al., 2024). It is found that RNNs with input delayed
106 time gave better predictive performances for multivariate reservoir inflow prediction than Input Delayed Neural
107 Network (IDNN) (Coulibaly et al., 2001). Real-time reservoir inflow prediction in the case of different climate
108 scenarios and lead time conditions (+1-Hr, +4-Hr, and +6-Hr) with three conventional ML algorithms; (1) SVM, (2)
109 RF, (3) MLP and four DL algorithms; (1) DNNs, (2) RNNs, (3) LSTM, (4) GRU were investigated. In comparison,
110 the results distinctly showed that DNNs outperformed than the conventional ANNs in most scenarios. However, under
111 the extended periods of lead time prediction, underestimation of reservoir inflow by DNNs is more serious compared
112 to ANNs (Huang et al., 2022). Encoder-Decoder LSTM (ED-LSTM) was employed for sub-seasonal reservoir inflow
113 with multiple lead time (+1-D to +30-D) for 30 reservoirs, at 1-D ahead prediction, ED-LSTM could produce good
114 predictive performance of NSE exceeding 0.75 for 29 reservoirs. At 30-D ahead prediction, ED-LSTM achieved NSE
115 of more than 0.5 for most reservoirs (Fan et al., 2023). Furthermore, LSTM exhibited superior performances in



116 predicting medium to long-term data compared to the conventional ML algorithms as well as RNNs (Khorram and
117 Jehbez, 2023; Rajesh et al., 2023) and CNNs architectures (Herbert et al., 2021).

118 However, the biased performance of overfitting, information saturation, and under-fitting issues of ML-
119 based prediction models has become the challenging issues. It is reviewed that ML models cannot improve the
120 prediction accuracy without including preprocessing techniques for feature engineering (Apaydin and Sibtain, 2021).
121 Data preprocessing is conducted at the first step of ML modeling to ensure the data quality for model training. Data
122 cleaning, transformation, and decomposition are adopted for prediction improvement. In addition, selecting suitable
123 ML algorithms for specific purpose of hydrological prediction is a challenging task.

124 This study employed two powerful ML algorithms; XGBoost and LSTM for univariate and multivariate
125 reservoir inflow prediction of two large storage dams in the Chao Phraya River Basin (CPYRB); (1) Bhumibol (BB)
126 and Sirikit (SK) dams as shown in Fig. 1. Predicting precise and accurate reservoir inflow for these two reservoirs
127 is important to ensure reliable water supply sources and establish proper water allocation plan for the downstream water
128 use in the central region. Furthermore, during the storm seasons from May, to Dec. when the flood risks are likely
129 elevated, future inflow data is informative for the Office of National Water Resources (ONWR), key decision maker
130 to implement effective flood mitigation strategies. Input features selection and configuration design of two different
131 types of daily and monthly reservoir inflow prediction models; (1) univariate prediction with XGBoost and LSTM
132 algorithms and (2) multivariate prediction with LSTM algorithm, were definitely highlighted. In the last step,
133 predictability of predicting low and high reservoir inflow values of these models were accordingly explored to assess
134 their statistical performances.

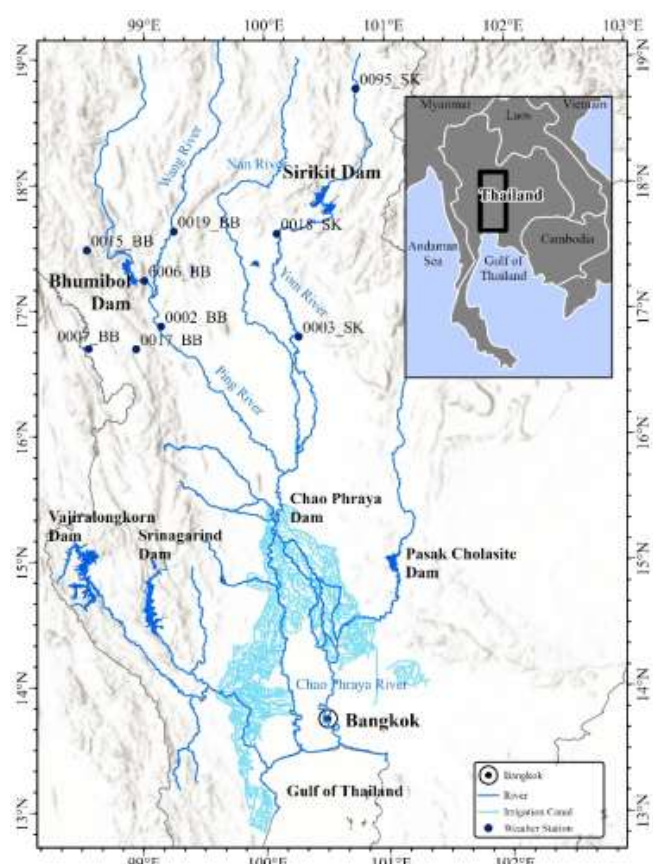


Fig. 1 Study area in the Chao Phraya River Basin and weather stations



137 2. Material and methods

138

139 **2.1. Input features for reservoir inflow prediction models**

140 The development of ML prediction models relied on the historical observation data from 2000 to 2020
141 including reservoir inflows of BB and SK reservoirs, and climate data gathered from the nearest weather stations as
142 summarized in Table 1. As input feature selection is definitely critical to the success of ML- and DL-based prediction
143 models, consequently, the statistical correlation analysis was performed to assess the strength and direction of
144 relationships between climate data from adjacent weather stations and reservoir inflow. By doing this, the daily
145 observed climate data (air humidity, air pressure, temperature, and rainfall) was collected from six Thai Meteorological
146 Department (TMD) stations (0002, 0006, 0007, 0015, 0017, and 0019) located in Tak, Sukhothai, and Lampang
147 provinces near BB dam. Additionally, climate data from the Climate Data Services (CDS) publicly provided by NASA
148 was gathered for locations with geographic coordinates matching those of the TMD stations. Likewise, the daily
149 observed climate data near SK dam was collected from three TMD and NASA stations (0003, 0018, and 0095) located
150 in Phitsanulok, Uttaradit, and Nan provinces, respectively.

151 For the univariate prediction, single reservoir inflows of BB and SK dams were aimed to individually predict
152 for both daily and monthly models. A number of daily and monthly prediction scenarios with different model
153 configuration using XGBoost and LSTM algorithms were accordingly developed. For the multivariate prediction,
154 reservoir inflows of two main reservoirs, BB-SK dams were expected to achieve simultaneously from single
155 prediction model for both daily and monthly prediction. Consequently, LSTM was selected for multiple output
156 prediction as it can learn and capture the complicated relationship of relevant multiple input variables.

157

158 **Table 1** Data used for reservoir inflow prediction modelling

| Data | Description | Data Type | Unit | Data Length | | |
|---------------------|--------------------------------------|----------------------------|----------------------|---------------------|--|--|
| Reservoir Inflow_BB | Reservoir Inflow of BB Dam | Daily, Monthly | MCM | 1/1/2000–31/12/2020 | | |
| Reservoir Inflow_SK | Reservoir Inflow of PS Dam | Daily, Monthly | MCM | 1/1/2000–31/12/2020 | | |
| Weather | Avg. Humidity at 9 Stations | Daily, Monthly | % | 1/1/2000–31/12/2020 | | |
| | Avg. Air Pressure at 9 Stations | Daily, Monthly | hPa | 1/1/2000–31/12/2020 | | |
| | Avg. Temperature at 9 Stations | Daily, Monthly | °C | 1/1/2000–31/12/2020 | | |
| | Rainfall at 9 Stations at 9 Stations | Daily, Monthly | mm | 1/1/2000–31/12/2020 | | |
| | Station ID | Station Name | Location: Lat.–Long. | | | |
| 0002_BB | Tak | N 16°52'48" – E 99°08'24" | | | | |
| 0006_BB | Bhumibol Dam | N 17°14'37" – E 99°00'08" | | | | |
| 0007_BB | Mae Sot | N 16°41'60" – E 98°32'31" | | | | |
| 0015_BB | Si Samrong | N 17°29'11" – E 99°31'36" | | | | |
| 0017_BB | Doi Muser | N 16°41'60" – E 98°56'07" | | | | |
| 0019_BB | Tone | N 17°38'12" – E 99°14'44" | | | | |
| 0003_SK | Phitsanulok | N 16°47'47" – E 100°16'33" | | | | |
| 0018_SK | Uttaradit | N 17°37'00" – E 100°05'60" | | | | |
| 0095_SK | Nan | N 18°46'01" – E 100°45'47" | | | | |

159 Note: meter above mean sea level– m. msl.|Million Cubic Meter–MCM|Cubic Meter per Second–CMS

160

161 Selecting input features for each univariate and multivariate prediction model was based on the physical
162 river–reservoir system and statistical cross correlation between past reservoir inflow and relevant climate data as
163 summarized in Table 2. This ensured that the prediction model can effectively capture the strong relationship between
164 the inputs and predicted outputs.

165

166

167

168

169

170

171

172

173

174

175

176



177

Table 2 Correlation coefficient between climate data and reservoir inflows of the Bhumibol and Sirikit dams

| Weather Station | Climate Data | | TMD Data Source | NASA Data Source | Weather Station | Climate Data | | TMD Data Source | NASA Data Source |
|-----------------|-------------------------|--------------|-----------------|------------------|--|-------------------------|------------------------------------|-----------------|------------------|
| 0002_BB | Avg. humidity (%) | 0.402 | 0.521 | | 0019_BB | Avg. humidity (%) | 0.460 | 0.505 | |
| | Avg. air pressure (hPa) | -0.117 | -0.148 | | | Avg. air pressure (hPa) | -0.090 | -0.146 | |
| | Avg. temperature (°C) | -0.115 | -0.190 | | | Avg. temperature (°C) | -0.091 | -0.133 | |
| | Rainfall (mm/day) | 0.284 | 0.365 | | | Rainfall (mm/day) | 0.191 | 0.355 | |
| 0006_BB | Avg. humidity (%) | 0.402 | 0.518 | | 0003_SK | Avg. humidity (%) | 0.428 | 0.536 | |
| | Avg. air pressure (hPa) | -0.007 | -0.146 | | | Avg. air pressure (hPa) | -0.328 | -0.322 | |
| | Avg. temperature (°C) | -0.103 | -0.173 | | | Avg. temperature (°C) | -0.020 | -0.144 | |
| | Rainfall (mm/day) | 0.289 | 0.369 | | | Rainfall (mm/day) | 0.038 | 0.376 | |
| 0007_BB | Avg. humidity (%) | 0.401 | 0.491 | | 0018_SK | Avg. humidity (%) | 0.499 | 0.503 | |
| | Avg. air pressure (hPa) | -0.164 | -0.179 | | | Avg. air pressure (hPa) | -0.023 | -0.339 | |
| | Avg. temperature (°C) | -0.096 | -0.076 | | | Avg. temperature (°C) | -0.019 | -0.017 | |
| | Rainfall (mm/day) | 0.197 | 0.360 | | | Rainfall (mm/day) | 0.167 | 0.406 | |
| 0015_BB | Avg. humidity (%) | 0.319 | 0.521 | | 0095_SK | Avg. humidity (%) | 0.535 | 0.469 | |
| | Avg. air pressure (hPa) | -0.021 | -0.139 | | | Avg. air pressure (hPa) | -0.379 | -0.358 | |
| | Avg. temperature (°C) | -0.027 | -0.178 | | | Avg. temperature (°C) | 0.092 | 0.101 | |
| | Rainfall (mm/day) | 0.162 | 0.363 | | | Rainfall (mm/day) | 0.002 | 0.392 | |
| 0017_BB | Avg. humidity (%) | 0.212 | 0.491 | | Note: | | Thai Meteorological Department–TMD | | |
| | Avg. air pressure (hPa) | 0.003 | -0.479 | | National Aeronautics and Space Administration–NASA | | | | |
| | Avg. temperature (°C) | 0.006 | -0.076 | | | | | | |
| | Rainfall (mm/day) | 0.034 | 0.360 | | | | | | |

178

179 The correlation analysis revealed strong correlations between observed reservoir inflows and both humidity
 180 and rainfall at both BB and SK dams. The correlation coefficient between reservoir inflow of BB dam and humidity
 181 data at Station 0006 reaches up to 0.402 and 0.518 for TMD and NASA data sources, respectively. Rainfall data from
 182 Station 0006 also exhibited a strong correlation with reservoir inflow of BB dam, with correlation coefficients of
 183 0.2886 and 0.3693 for TMD and NASA data sources, respectively. The substantial correlation between reservoir
 184 inflow of SK dam and climate data from Station 0018 particularly from NASA data source, was apparently found
 185 with the correlation coefficient of 0.503 and 0.406 for humidity data and precipitation data, respectively. Based on
 186 these analysis, humidity and rainfall data were accordingly selected to specify input structures of ML- and DL-
 187 based prediction models. Autocorrelation of past reservoir inflow was also analyzed to identify optimal lag times and
 188 number of moving average parameters for input feature selection. This analysis revealed the importance of closer lag
 189 time (t to t-7) which exhibited high correlation coefficients exceeding 0.67 with the recent reservoir inflow data for
 190 both BB and SK dams. Accordingly, information of past reservoir inflows with closer lag time t to t-7 was
 191 incorporated into the structure of the prediction models to predict reservoir inflow at lead time t+1.

192 Following this analysis, four daily and monthly univariate prediction scenarios with various model
 193 configurations varying input features using XGBoost and LSTM algorithms for each of BB and SK dams; S1–S4,
 194 were designed. For the multivariate prediction model, two daily and monthly prediction scenarios; S5–S6, using
 195 LSTM algorithm were established. Major inputs of these prediction models are past reservoir inflow at time t, moving
 196 average of past reservoir inflow at time t-3 and t-7, rainfall at time t, and humidity at time t as summarized in Table
 197 3. It is illustrated that univariate models structured the specific individual inputs for single reservoir inflow prediction
 198 at lead time t+1. For example, the input features of daily reservoir inflow prediction for BB dam are BB past inflow
 199 at time t, moving average of BB past inflow at time t-3 and t-7, rainfall and humidity at time t collected from the
 200 nearest weather stations to BB dam. In contrast, the multivariate prediction models incorporate inputs of both BB and
 201 SK dams to predict two reservoir inflows at lead time t+1.

202

203

Table 3 Input features for univariate and multivariate reservoir inflow prediction models

| Prediction Model | Reservoir Inflow ID | Prediction Scenario | Model Type and Prediction Lead Time | Model No. | Input Features | | | | | |
|-----------------------|---------------------|---------------------|-------------------------------------|--|----------------|----------------|------------------|------------------|----------|----------|
| | | | | | Past Inflow_BB | Past Inflow_SK | Avg. Past Inflow | Avg. Past Inflow | Rainfall | Humidity |
| Univariate Prediction | BB | S1: XGBoost | Daily | dBB-01, dBB-02, dBB-03 | ✓ | – | ✓ | ✓ | ✓ | ✓ |
| | | S2: LSTM | Daily | dBB-01, dBB-02, dBB-03, dBB-04, dBB-05, dBB-06 | ✓ | – | ✓ | ✓ | ✓ | – |
| | SK | S1: XGBoost | Daily | dSK-01, dSK-02, dSK-03 | – | ✓ | ✓ | ✓ | ✓ | ✓ |



| Prediction Model | Reservoir Inflow ID | Prediction Scenario | Model Type and Prediction Lead Time | Model No. | Input Features | | | | | | |
|--|-------------------------|---------------------|--|------------------------|----------------|----------------|------------------|------------------|----------|----------|---|
| | | | | | Past Inflow_BB | Past Inflow_SK | Avg. Past Inflow | Avg. Past Inflow | Rainfall | Humidity | |
| — | — | — | t+1 | | t | t | t-3 | t-7 | t | t | |
| 204 205 206 207 208 209 210 211 212 213 214 215 216 217 218 219 220 221 222 223 224 225 226 227 228 229 230 231 232 233 234 235 236 237 | S2: LSTM | Daily | dSK-01, dSK-02, dSK-03, dSK-04, dSK-05, dSK-06 | | — | ✓ | ✓ | ✓ | ✓ | — | |
| | | | | | ✓ | — | ✓ | ✓ | ✓ | ✓ | |
| | BB | S3: XGBoost | Monthly | mBB-01, mBB-02, mBB-03 | ✓ | — | ✓ | ✓ | ✓ | ✓ | |
| | | | | | ✓ | — | ✓ | ✓ | ✓ | — | |
| | SK | S3: XGBoost | Monthly | mSK-01, mSK-02, mSK-03 | — | ✓ | ✓ | ✓ | ✓ | ✓ | |
| | | | | | — | ✓ | ✓ | ✓ | ✓ | — | |
| | Multivariate Prediction | BB&SK | S5: LSTM | Daily | dBBSK-01 | ✓ | ✓ | ✓ | — | ✓ | ✓ |
| | | BB&SK | S6: LSTM | Monthly | dBBSK-01 | ✓ | ✓ | ✓ | — | ✓ | ✓ |

Note: Acronyms—Bhumibol dam—BB|Sirikit dam—SK|Daily Univariate prediction model of BB dam—dBB|Daily univariate prediction model of SK Dam—dSK|Daily multivariate prediction model of BB&SK dams—dBBSK|Monthly multivariate prediction model of BB&SK dams—mBBSK

2.2. Prediction algorithms selected

2.2.1. Extreme gradient boosting (XGBoost)

Extreme Gradient Boosting (XGBoost), a powerful machine learning algorithm initiated by Tianqi Chen in 2014 (Chen and Guestrin, 2016), was used to develop the daily and monthly univariate prediction models for reservoir inflow in CPYRB. XGBoost is a decision-tree-based ensemble machine learning as illustrated its structure in Fig. 2. Its efficiency, scalability, and flexibility have been widely demonstrated and proven in hydrological prediction applications (Rajesh et al., 2022). In general, the supervised XGBoost learning primarily involves minimizing objective function which consists of two main components; (1) loss function and (2) regularization term as expressed in Eq. (1). This loss function measures the discrepancy between the predicted and observed values in the model training process as given mean squared error in Eq. (2). The regularization term in Eq. (3) is crucial in preventing model overfitting and complexity for improved prediction performance.

$$Obj(\theta) = L(\theta) + \mathcal{Q}(\theta) \quad (1)$$

$$L(\theta) = \frac{1}{2} \sum_{i=1}^n (y_i - p_i)^2 \quad (2)$$

$$\mathcal{Q}(\theta) = \gamma T + \frac{1}{2} \lambda \sum_{i=1}^T O_{value}^2 \quad (3)$$

where, $L(\theta)$ is the training loss function term. For robust regression tasks, the common loss functions are Mean Squared Error (MSE), Mean Absolute Error (MAE), and Huber loss which is the combination of MSE and MAE. $\mathcal{Q}(\theta)$ is regularization term. θ denotes the optimal parameter values that best fits the training inflow data (y_i) to the predicted inflow output (p_i). γ is a hyperparameter controlling the strength of the regularization term which influences the decision to make a further partition on a leaf node of a tree-based model. T is a number of leaf nodes in the tree and λ is a hyperparameter used to scale the regularization term. A larger number of leaf nodes signifies the model complexity potentially leading to overfitting. A larger λ indicates the increased penalty to model encouraging the reduction of model complexity. O_{value} is a measure of the impurity or heterogeneity of the data points within the leaf node. For tree building process, a prediction for one given data is made by traversing the tree from the root node to a leaf node. The tree is built from a root node and recursively split into left and right child nodes. This process continues until a specific stopping criterion is met as graphically shown in Fig. 2. Similarity score (Sim) is used to assess the homogeneity of data within a node to guide for leaf node splitting. The larger value of similarity score signifies the similar data within a leaf node that further splitting might not be necessary. Similarity score is computed to indicate a score of each node by using Eq. (4).



238

239 Gain value is termed to measure the accuracy improvement resulted from a specific splitting. It helps assess
 240 the optimality of potential splits in a tree structure as expressed in Eq. (5). A higher positive gain value indicates a
 241 better split in improving the model predictive performance. When the gain values are negative, the tree branch is
 242 removed as shown in Fig. 3.

243

244

245 where, $Simleft$, $Simright$, and $Simroot$ denote the similarity score of the left leaf node, right leaf node, and
 246 root node of the branch, respectively. The tree structures are iteratively built for T iterations until the desired number
 247 of models is reached. In each iteration, the output value (O_{value}) for all leaf nodes is computed using Eq. (6).

248

249

250 In addition, the precision and speed of convergence of the prediction model is governed by learning rate (ϵ).
 251 Learning rate determines level of model improvement to handle the prediction error made by previous iterations. A
 252 larger values of learning rate can accelerate the training process leading to faster convergence. However, overfitting
 253 can simply find if not properly fine-tuned. In contrast, the smaller values of learning rate can help reduce overfitting
 254 but speed of convergence is definitely lower. In the final step, XGBoost can make updated prediction (p_i^t) by combining
 255 the initial prediction (p_i^0) with the gradient of the loss function and the regularization term multiplied with learning
 256 rate as expressed in Eq. (7).

257

258

$$Sim = \frac{\sum_{i=1}^n (y_i - p_i)^2}{n + \lambda} \quad (4)$$

$$Gain\ value = (Simleft + Simright) - Simroot \quad (5)$$

$$O_{value} = \frac{\sum_{i=1}^n (y_i - p_i)^2}{n + \lambda} \quad (6)$$

$$p_i^t = p_i^0 + \epsilon [\sum_{i=1}^n L(y_i, p_i^0 + O_{value}) + \frac{1}{2} \lambda O_{value}^2] \quad (7)$$

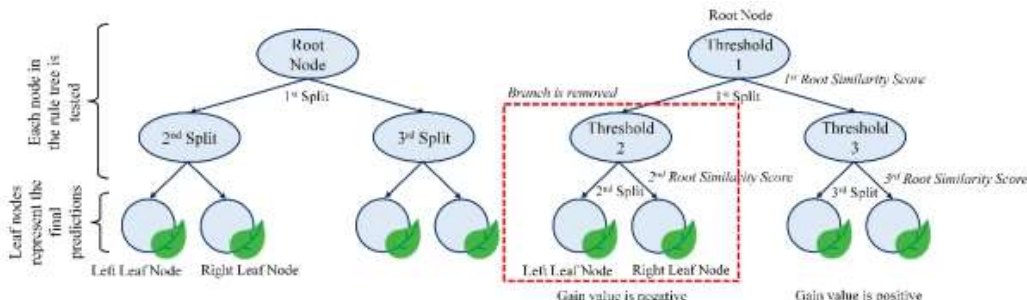


Fig. 2 XGBoost tree-based structure

259

260

2.2.2. Long Short-Term Memory (LSTM)

261 Long Short-Term Memory (LSTM) is a well-suited type of deep learning algorithm designed to process
 262 sequential data. It was initially introduced by Hochreiter and Schmidhuber in 1997 (Hochreiter and Schmidhuber,
 263 1997). LSTM is an evolution of Recurrent Neural Networks (RNN) which is a type of Artificial Neural Networks
 264 (ANNs) having memory to process sequential inputs. However, the complications to learn and capture long-term
 265 dependencies due to vanishing and exploding gradient problems become the significant drawback of RNN. To
 266 overcome this, LSTM is specifically developed to learn long-term dependencies and retain previous information over
 267 extended periods. The LSTM model is commonly structured as a chain of units as illustrated in Fig. 3. Each LSTM
 268 unit is composed of a cell state and three gates namely, (1) input gate, (2) forget gate, and output gate. Cell state is
 269 functioned as core component of LSTM to store and carry information through time steps. Input gate regulates new
 270 information from current input to be stored in a cell state. Forget gate decides to discard or keep information from
 271 previous cell state. Output gate determines which part of cell state should be the current prediction output (Khorram
 272 and Jehbez, 2023; Rajesh et al., 2023).



273 In the initial step, forget gate examines the current input at time t (x_t), previous hidden state (h_{t-1}) which is
 274 the output at previous time $t-1$, and long-term memory from previous cell state at time $t-1$ (C_{t-1}). It calculates a value
 275 in a range of 0 and 1 for each element in the previous cell state as expressed in Eq. (8). Subsequently, the input gate
 276 calculates two values; input gate at time t (i_t) and cell state input at time t (\tilde{C}_t) to regulate the new information into the
 277 current cell state as defined in Eq. (9) and Eq. (10). Then, the new cell state at time t (C_t) in Eq. (11) is updated by
 278 combining the new information of previous cell state at time $t-1$ (C_{t-1}), forget gate at time t (f_t), and input gate at time
 279 t (i_t, \tilde{C}_t). Eq. (12) is employed to compute the current prediction output at time t (o_t). The hidden state (h_t) indicating
 280 LSTM output at time t , is finally calculated by multiplying the output gate at time t (o_t) with the tanh of the new cell
 281 state at time t (C_t) as shown in Eq. (12) and Eq. (13). By doing this through iteration process, LSTM can handle the
 282 sequential data and make accurate and precise prediction.

283

$$f_t = \sigma(W_f * [h_{t-1}, x_t] + b_f) \quad (8)$$

$$i_t = \sigma(W_i * [h_{t-1}, x_t] + b_i) \quad (9)$$

$$\tilde{C}_t = \tanh(W_C * [h_{t-1}, x_t] + b_C) \quad (10)$$

$$C_t = f_t * C_{t-1} + i_t * \tilde{C}_t \quad (11)$$

$$o_t = \sigma(W_o * [h_{t-1}, x_t] + b_o) \quad (12)$$

$$h_t = o_t * \tanh(C_t) \quad (13)$$

284

285

286 Where $W_{f/i/C}$ is corresponding weight matrix, $b_{f/i/C}$ is corresponding bias and σ is the sigmoid activation
 287 function.

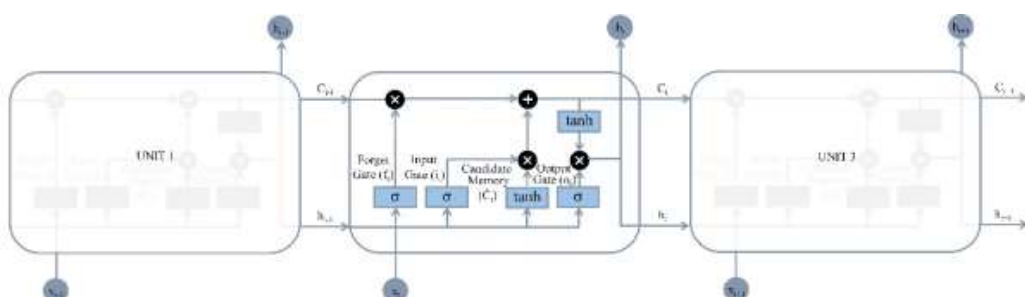


Fig. 3 LSTM chain-like structure and its unit

288

289

2.3. Model configuration design and prediction modelling

290 Model configuration design of daily and monthly univariate and multivariate prediction models are presented
 291 in Fig. 4 and Table 4–Table 5. The input features as aforementioned in Section 2.1., designated training–testing dataset
 292 ratios (60:40, 70:30, 80:20), delayed time of moving average inflow (t–3 and t–7), and learning rates (0.001, 0.01, 0.1)
 293 were varied to optimize the model configuration and prediction performance. Implementation of training model for
 294 daily and monthly prediction by XGBoost was controlled by the hyperparameter tuning process such as gamma,
 295 maximum depth of a tree, number of iterations (nrounds), number of threads (nthreads), learning rate, number of fold
 296 (nfolds) and early stopping rounds (early_stopping_rounds) parameters as presented in Table 4. In this study,
 297 maximum depth of a tree was set to 6 to increase deeper tree model complexity. Maximum number of iterations was
 298 specified to 10,000 for model training process. Number of threads determining for parallel computation to speed up
 299 the training process and number of folds specifying for cross-validation was 10 and 2, respectively. The early stopping
 300 rounds were generally used to stop training procedures when the loss on training dataset starts increasing. In this study,
 301 the early stopping round was set every 500 iterations if the performance on RMSE was not substantially improved.

302

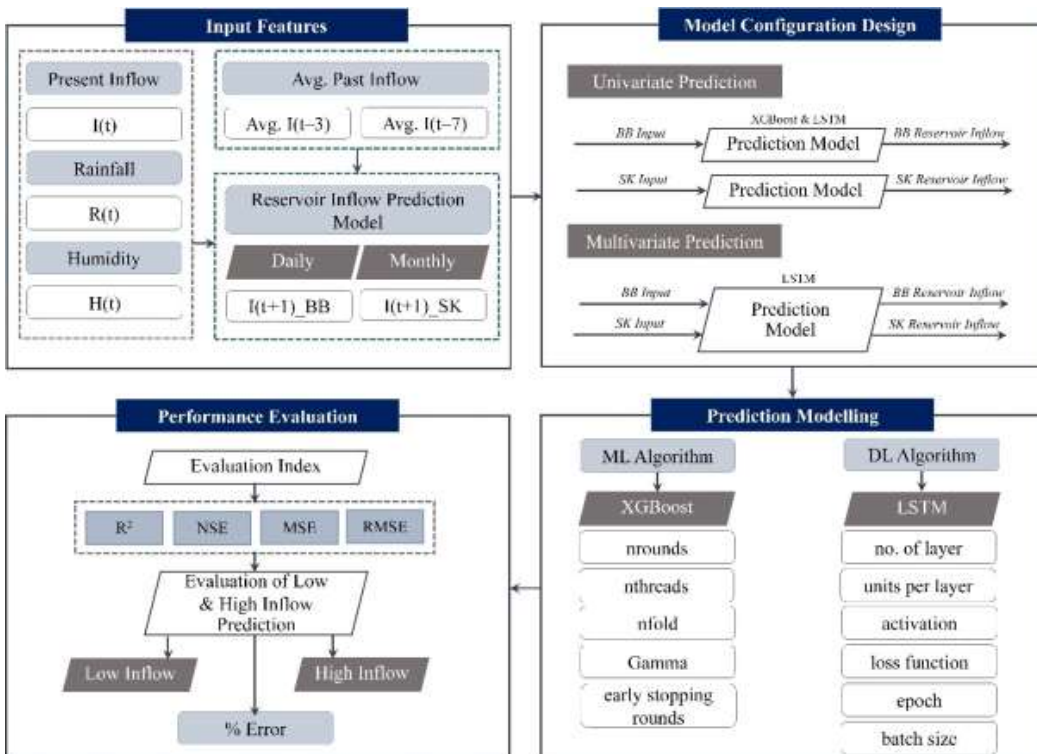


Fig. 4 Workflow diagram of this study

303
 304

Table 4 Model configuration design of daily and monthly univariate prediction models using XGBoost

| Model No. | Input Feature | Training:Testing Ratio | Learning Rate | XGBoost Parameter | | | | | | | |
|---|---|------------------------|------------------|--------------------|-------|------------|------------|---------|----------|--------|-----------------------|
| | | | | Objective | Gamma | Max. Depth | Evaluation | nrounds | nthreads | nfolds | Early stopping rounds |
| Daily and Monthly Prediction of BB Reservoir Inflow | | | | | | | | | | | |
| dBB-01, mBB-01 | Past Inflow, Avg. Past Inflow | 60:40, 70:30, 80:20 | 0.001, 0.01, 0.1 | regression: linear | 0 | 6 | RMSE | 10,000 | 10 | 2 | 500 |
| dBB-02, mBB-02 | Past Inflow, Avg. Past Inflow, Rainfall | 60:40, 70:30, 80:20 | 0.001, 0.01, 0.1 | regression: linear | 0 | 6 | RMSE | 10,000 | 10 | 2 | 500 |
| dBB-03, mBB-03 | Past Inflow, Avg. Past Inflow, Rainfall, Humidity | 60:40, 70:30, 80:20 | 0.001, 0.01, 0.1 | regression: linear | 0 | 6 | RMSE | 10,000 | 10 | 2 | 500 |
| Daily and Monthly Prediction of SK Reservoir Inflow | | | | | | | | | | | |
| dSK-01, mSK-01 | Past Inflow, Avg. Past Inflow | 60:40, 70:30, 80:20 | 0.001, 0.01, 0.1 | regression: linear | 0 | 6 | RMSE | 10,000 | 10 | 2 | 500 |
| dSK-02, mSK-02 | Past Inflow, Avg. Past Inflow, Rainfall | 60:40, 70:30, 80:20 | 0.001, 0.01, 0.1 | regression: linear | 0 | 6 | RMSE | 10,000 | 10 | 2 | 500 |
| dSK-03, mSK-03 | Past Inflow, Avg. Past Inflow, Rainfall, Humidity | 60:40, 70:30, 80:20 | 0.001, 0.01, 0.1 | regression: linear | 0 | 6 | RMSE | 10,000 | 10 | 2 | 500 |

305



306 Similarly, model configuration using LSTM for both univariate and multivariate prediction models was
 307 designed by varying input features and tuning key hyperparameters such as number of layers, number of units per
 308 layer, activation function, optimizer, epoch, and batch size, etc. as summarized in Table 5. In this study, number of
 309 layers was set to 2 and units per layer referring number of neurons in a specific layer of LSTM network was set to 64
 310 or 32. Rectified Linear Unit (ReLU), a famous activation function used in deep neural networks was specified in all
 311 univariate prediction experiments while Sigmoid, a traditional activation function was used for multivariate prediction.
 312 Adam optimizer which is an optimization algorithm, was employed to update weights during training process. MSE
 313 was used as loss function for both univariate and multivariate prediction models. Additionally, number of epochs
 314 involving the passing numbers through the entire training dataset was varied between 50, 100, and 500. Similarly,
 315 batch size incorporating number of samples processed before updating the model's weights was set to 16, 32, and 64.
 316

317 **Table 5** Model configuration design of daily and monthly univariate and multivariate prediction models using LSTM

| Model No. | Input Feature | Standardization Technique | LSTM Parameter in Keras | | | | | | | |
|--|---|---------------------------|-------------------------|------------------|-----------------|------------|---------------|-----------|-------|------------|
| | | | Steps | Number of Layers | Units per Layer | Activation | Loss Function | Optimizer | Epoch | Batch Size |
| Daily Univariate Prediction Models of BB Dam | | | | | | | | | | |
| dBB-01 | Past Inflow, Avg. Past Inflow | Standard | 3 | 2 | 64/32 | ReLU | MSE | Adam | 50 | 16 |
| dBB-02 | Past Inflow, Avg. Past Inflow | Standard | 7 | 2 | 64/32 | ReLU | MSE | Adam | 50 | 16 |
| dBB-03 | Past Inflow, Avg. Past Inflow | Standard | 14 | 2 | 64/32 | ReLU | MSE | Adam | 50 | 16 |
| dBB-04 | Past Inflow, Avg. Past Inflow, Rainfall | Standard | 3 | 2 | 64/32 | ReLU | MSE | Adam | 50 | 16 |
| dBB-05 | Past Inflow, Avg. Past Inflow, Rainfall | Standard | 7 | 2 | 64/32 | ReLU | MSE | Adam | 50 | 16 |
| dBB-06 | Past Inflow, Avg. Past Inflow, Rainfall | Standard | 14 | 2 | 64/32 | ReLU | MSE | Adam | 50 | 16 |
| Daily Univariate Prediction Models of SK Dam | | | | | | | | | | |
| dSK-01 | Past Inflow, Avg. Past Inflow | Standard | 3 | 2 | 64/32 | ReLU | MSE | Adam | 50 | 16 |
| dSK-02 | Past Inflow, Avg. Past Inflow | Standard | 7 | 2 | 64/32 | ReLU | MSE | Adam | 50 | 16 |
| dSK-03 | Past Inflow, Avg. Past Inflow | Standard | 14 | 2 | 64/32 | ReLU | MSE | Adam | 50 | 16 |
| dSK-04 | Past Inflow, Avg. Past Inflow, Rainfall | Standard | 3 | 2 | 64/32 | ReLU | MSE | Adam | 50 | 16 |
| dSK-05 | Past Inflow, Avg. Past Inflow, Rainfall | Standard | 7 | 2 | 64/32 | ReLU | MSE | Adam | 50 | 16 |
| dSK-06 | Past Inflow, Avg. Past Inflow, Rainfall | Standard | 14 | 2 | 64/32 | ReLU | MSE | Adam | 50 | 16 |
| Monthly Univariate Prediction Models of BB Dam | | | | | | | | | | |
| mBB-01 | Past Inflow, Avg. Past Inflow | MinMax | 3 | 2 | 64/32 | ReLU | MSE | Adam | 100 | 16 |
| mBB-02 | Past Inflow, Avg. Past Inflow | MinMax | 3 | 2 | 64/32 | ReLU | MSE | Adam | 100 | 32 |
| mBB-03 | Past Inflow, Avg. Past Inflow | MinMax | 3 | 2 | 64/32 | ReLU | MSE | Adam | 100 | 64 |
| mBB-04 | Past Inflow, Avg. Past Inflow, Rainfall | MinMax | 3 | 2 | 64/32 | ReLU | MSE | Adam | 100 | 16 |
| mBB-05 | Past Inflow, Avg. Past Inflow, Rainfall | MinMax | 3 | 2 | 64/32 | ReLU | MSE | Adam | 100 | 32 |
| mBB-06 | Past Inflow, Avg. Past Inflow, Rainfall | MinMax | 3 | 2 | 64/32 | ReLU | MSE | Adam | 100 | 64 |
| Monthly Univariate Prediction Models of SK Dam | | | | | | | | | | |
| mSK-01 | Past Inflow, | MinMax | 3 | 2 | 64/32 | ReLU | MSE | Adam | 100 | 16 |



| Model No. | Input Feature | Standardization Technique | LSTM Parameter in Keras | | | | | | | |
|---|--|---------------------------|-------------------------|------------------|-----------------|------------|---------------|-----------|-------|------------|
| | | | Steps | Number of Layers | Units per Layer | Activation | Loss Function | Optimizer | Epoch | Batch Size |
| | Avg. Past Inflow | | | | | | | | | |
| mSK-02 | Past Inflow, Avg. Past Inflow | MinMax | 3 | 2 | 64/32 | ReLU | MSE | Adam | 100 | 32 |
| mSK-03 | Past Inflow, Avg. Past Inflow | MinMax | 3 | 2 | 64/32 | ReLU | MSE | Adam | 100 | 64 |
| mSK-04 | Past Inflow, Avg. Past Inflow, Rainfall | MinMax | 3 | 2 | 64/32 | ReLU | MSE | Adam | 100 | 16 |
| mSK-05 | Past Inflow, Avg. Past Inflow, Rainfall | MinMax | 3 | 2 | 64/32 | ReLU | MSE | Adam | 100 | 32 |
| mSK-06 | Past Inflow, Avg. Past Inflow, Rainfall | MinMax | 3 | 2 | 64/32 | ReLU | MSE | Adam | 100 | 64 |
| Daily and Monthly Multivariate Prediction Models of BB-SK Dam | | | | | | | | | | |
| dBBSK-01, mBBSK-01, | BB Past Inflow, SK Past Inflow, BB Avg. Past Inflow, SK Avg. Past Inflow, BB Rainfall, SK Rainfall, BB Humidity, SK Humidity | MinMax | 3 | 2 | 64 | Sigmoid | MSE | Adam | 500 | 64 |

318

319

2.4. Evaluation of predictive performance

320

The statistical metrics; Coefficient of Determination (R^2), Nash–Sutcliffe Efficiency (NSE), Mean Squared Error (MSE), Root Mean Squared Error (RMSE), were used to evaluate the perfect match between the predicted and observation values of reservoir inflows. R^2 is statistical measures describing the degree of linear correlation between two independent variables which ranges from 0 to 1 (Al–Aqeeli et al., 2015). A higher R^2 value closer to 1 indicates better fit of the prediction model to the observation values making stronger predictive power. NSE is the normalized statistical measure that compares the relative magnitude of the model prediction errors to observed data variance ranging from $-\infty$ to 1 (Brownlee, 2018). The prediction accuracy can be classified into three main classes subject to NSE. When NSE is greater than or equal to 0.90, the prediction accuracy is classified as “Class A–Excellent”, NSE ranges between 0.70 and 0.90, it is considered as “Class B–Good), and NSE lies between 0.50 and 0.70, it is classified as “Class C–Moderate” (China National Standardization Management Committee, 2008; Zhang et al., 2021). MSE, and RMSE metrics quantify the absolute and squared differences between the predicted and actual values, respectively. A lower value of MSE, and RMSE indicates better model performance. A prediction model is considered as precise and robust prediction when R^2 and NSE values are relatively approach to 1, MSE and RMSE values are small.

333

In the last step, the predictability to predict the low, average, and high daily and monthly reservoir inflows of BB and SK dams was assessed to leverage the application of ML–and DL–based prediction model for real–time reservoir operation and planning during the critical periods. The lowest, average, and highest reservoir inflows of the tested results were compared to the observed reservoir inflows. Finally, percentage error in prediction was computed.

337

3. Results and Discussion

338

3.1. Predicted one–day and one–month ahead of BB and SK reservoir inflows

339

In this study, R^2 and NSE were prioritized over MSE and RMSE to identify the optimal predictive model performances on the training and testing datasets. The quantitative and qualitative comparisons between observed and predicted inflows of the optimal daily and monthly univariate and multivariate prediction models for six scenarios are presented in Table 6 and illustrated in Fig. 5 and Fig. 6. The qualitative results from 2000 to 2020 demonstrated that daily and monthly predicted inflows for both BB and SK dams closely matched the observed inflows for both training and testing datasets when univariate and multivariate prediction models were performed. Even the monthly inflow pattern obtained from univariate and multivariate prediction models are likely similar to observed values, however, monthly prediction exhibited larger deviation from the observed values compared to daily prediction particularly the lowest and highest reservoir inflows.

340

341

342

343

344

345

346

347

348

349



350

Table 6 The optimal predictive performances of daily and monthly reservoir inflow prediction

| Scenario Design | Model Building | Univariate Prediction Model | | | Scenario Design | Model Building | Multivariate Prediction Model | | |
|---|----------------|-----------------------------|---------|---------|--|----------------|-------------------------------|---------|---------|
| | | Statistical Metrics | BB | SK | | | Statistical Metrics | BB | SK |
| S1: Daily model using XGBoost algorithm | Training | R^2 | 0.922 | 0.884 | S5: Daily model using LSTM algorithm | Training | R^2 | 0.894 | 0.842 |
| | | NSE | 0.909 | 0.871 | | | NSE | 0.890 | 0.841 |
| | | MSE | 62.919 | 70.000 | | | MSE | 75.698 | 97.183 |
| | | RMSE | 7.932 | 8.367 | | | RMSE | 8.700 | 9.858 |
| | Testing | R^2 | 0.885 | 0.836 | | Testing | R^2 | 0.873 | 0.780 |
| | | NSE | 0.862 | 0.816 | | | NSE | 0.857 | 0.767 |
| | | MSE | 31.990 | 81.308 | | | MSE | 36.039 | 92.455 |
| | | RMSE | 5.656 | 9.017 | | | RMSE | 6.003 | 9.615 |
| S2: Daily model using LSTM algorithm | Training | R^2 | 0.925 | 0.878 | S6: Monthly model using LSTM algorithm | Training | R^2 | 0.542 | 0.518 |
| | | NSE | 0.924 | 0.878 | | | NSE | 0.538 | 0.512 |
| | | MSE | 46.898 | 61.577 | | | MSE | 183,353 | 192,778 |
| | | RMSE | 6.848 | 7.847 | | | RMSE | 428 | 439 |
| | Testing | R^2 | 0.827 | 0.851 | | Testing | R^2 | 0.526 | 0.487 |
| | | NSE | 0.818 | 0.851 | | | NSE | 0.397 | 0.459 |
| | | MSE | 60.770 | 67.050 | | | MSE | 103,050 | 130,290 |
| | | RMSE | 7.800 | 8.190 | | | RMSE | 321 | 361 |
| S3: Monthly model using XGBoost algorithm | Training | R^2 | 0.452 | 0.490 | | | | | |
| | | NSE | 0.411 | 0.473 | | | | | |
| | | MSE | 217,267 | 196,562 | | | | | |
| | | RMSE | 466 | 443 | | | | | |
| | Testing | R^2 | 0.679 | 0.520 | | | | | |
| | | NSE | 0.675 | 0.513 | | | | | |
| | | MSE | 65,836 | 128,363 | | | | | |
| | | RMSE | 257 | 358 | | | | | |
| S4: Monthly model using LSTM algorithm | Training | R^2 | 0.519 | 0.678 | | | | | |
| | | NSE | 0.513 | 0.673 | | | | | |
| | | MSE | 186,719 | 104,617 | | | | | |
| | | RMSE | 432 | 323 | | | | | |
| | Testing | R^2 | 0.388 | 0.434 | | | | | |
| | | NSE | 0.353 | 0.407 | | | | | |
| | | MSE | 122,597 | 158,222 | | | | | |
| | | RMSE | 350 | 398 | | | | | |

351
 352

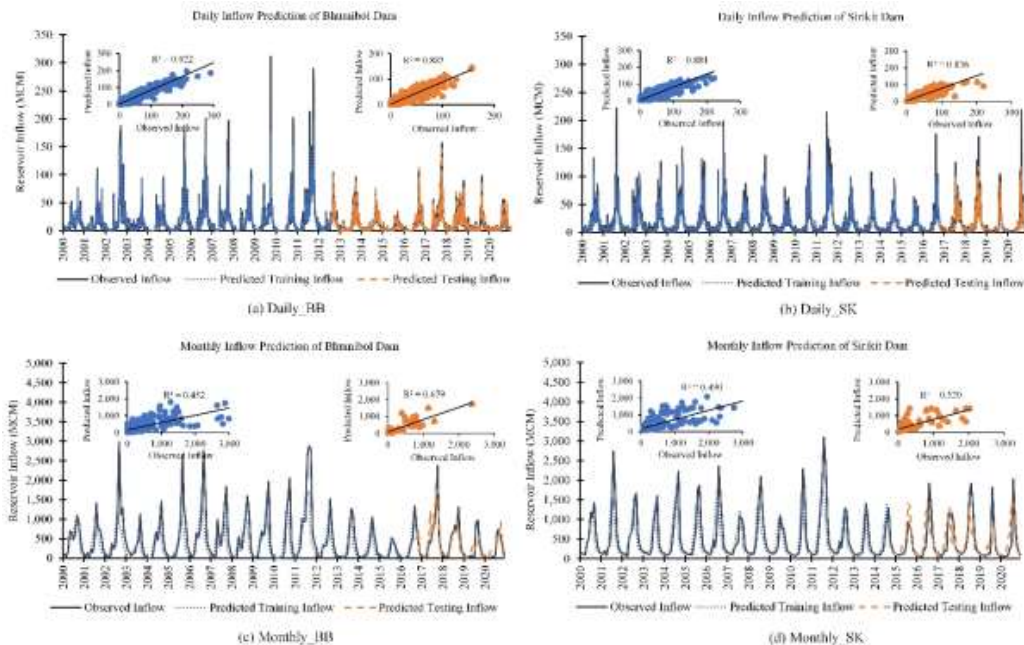


Fig. 5 Optimal predictive performances of one-day and one-month ahead univariate prediction models of BB and SK reservoir inflows

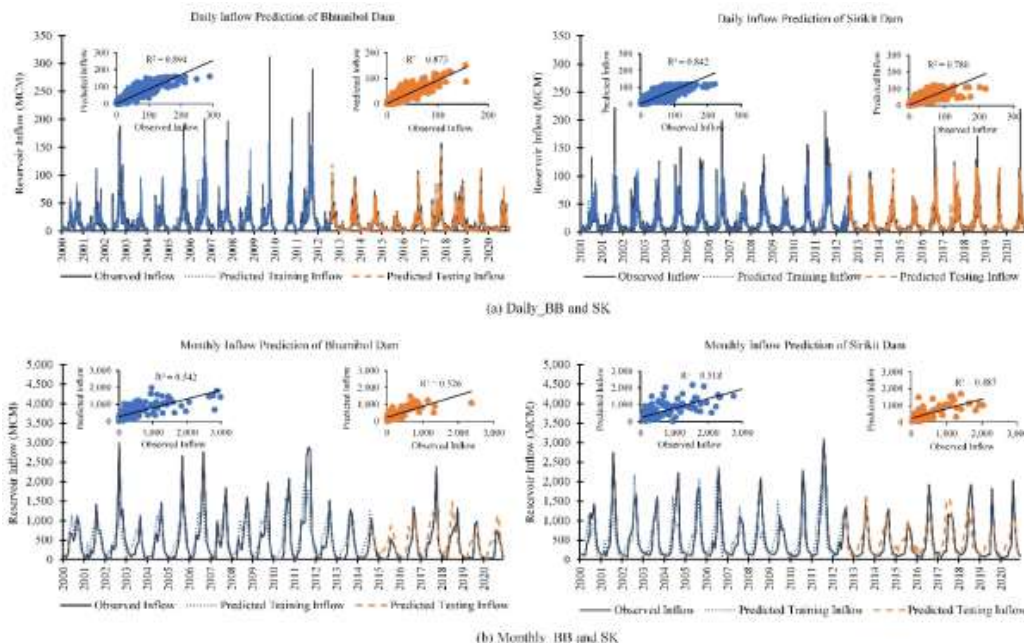


Fig. 6 Optimal predictive performances of one-day and one-month ahead multivariate prediction models of BB and SK reservoir inflows



353 Fig. 7 and Fig. 8 quantitatively illustrate the performance metrics of all scenarios of 1-day ahead and 1–
354 month ahead reservoir inflow predictions for both univariate and multivariate predictions. For the daily univariate
355 prediction using XGBoost on the training dataset, Scenario 1 (S1) achieved R^2 and NSE values of 0.922 and 0.909 for
356 BB dam and 0.884 and 0.871 for SK dam, respectively. However, R^2 and NSE values were slightly lower on the testing
357 dataset with the values of 0.885 and 0.862 for BB dam and 0.836 and 0.816 for SK dam, respectively. MSE and RMSE
358 values for BB dam were likely lower by -49.16% and -28.68% when 20% of dataset was accordingly tested. In
359 contrast, these two values were slightly increased on the testing dataset for SK dam by +16.15% and +7.77%. It is
360 revealed that the daily univariate prediction using LSTM (Scenario 2, S2) on the training dataset mostly demonstrated
361 higher R^2 and NSE values of 0.925 and 0.924 for BB dam and 0.878 and 0.878 for SK dam, respectively indicating
362 slightly higher predictive performances than XGBoost. Similar to XGBoost, R^2 and NSE values slightly decreased on
363 the testing dataset achieving 0.827 and 818 for BB dam. For SK dam, these two statistical metrics considerably
364 increased to 0.851 and 0.851 for SK dam, respectively. However, MSE and RMSE values performed by LSTM were
365 +29.58% and +13.90% for BB dam and +8.89% and +4.37% for SK dam which were lower than XGBoost,
366 respectively. For the Scenario 5 (S5) when daily multivariate prediction model was executed using LSTM to predict
367 reservoir inflow for both BB and SK dams, R^2 and NSE values of training dataset were 0.894 and 0.890 for BB dam
368 and 0.842 and 0.841 for SK dam, respectively. These values were slightly lower than those trained by daily univariate
369 prediction model using both XGBoost and LSTM. On the testing dataset with daily multivariate prediction model, R^2
370 and NSE values for BB dam were slightly higher than those obtained by daily univariate prediction model for both
371 XGBoost and LSTM, reaching 0.873 and 0.857, respectively. However, these values decreased considerably to 0.780
372 and 0.767, respectively for SK dam. In terms of MSE and RMSE, there was an insubstantial difference between
373 univariate and multivariate prediction models.

374 The predictive results exhibited that the predictability of daily univariate prediction models is slightly
375 superior than multivariate models, as they were developed independently to extract the specific input features of each
376 dam. However, the daily multivariate prediction model could provide two predictive outputs relatively closer to daily
377 univariate prediction model which is beneficial for real-time operational applications in the river basin. Due to the
378 high complexity of all input features and larger dataset used in the daily multivariate prediction model, however, DL-
379 based prediction model with LSTM algorithm could perform well in learning and capturing the input–output relation
380 and features, resulting in providing predictive performance closer to those achieved by the daily univariate prediction
381 model. Training larger datasets with LSTM for both daily univariate and multivariate prediction models gave the better
382 predictive performances than XGBoost. However, when smaller testing datasets were tested by LSTM, statistical
383 performance was slightly decreased compared to training dataset as obviously presented in Scenario 2 and Scenario
384 5. It is also revealed that daily reservoir inflow predictions for BB dam demonstrated higher performance compared
385 to SK dam, for both daily univariate and multivariate models. In comparison between XGBoost and LSTM for daily
386 reservoir inflow prediction on tested datasets, individual XGBoost model outperformed LSTM models across both
387 univariate and multivariate predictions for BB dam. For SK dam, the individual LSTM prediction model could predict
388 better results than the individual XGBoost model and the LSTM multivariate prediction model.

389
390

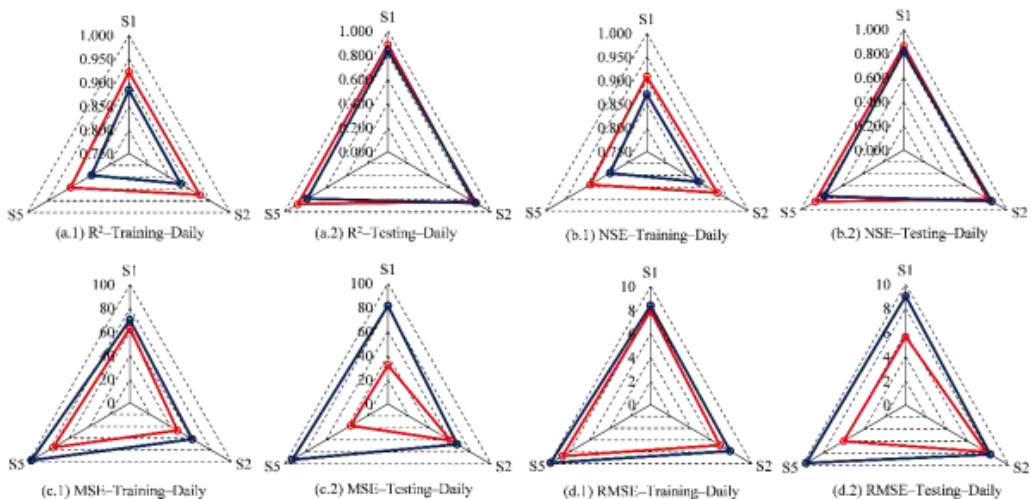


Fig. 7 Radar chart illustrating the performance metrics of all scenarios of 1-day ahead reservoir inflow prediction
(Legend: Red–BB, Blue–SK)

391

392

For ML-based monthly univariate prediction using XGBoost, Scenario 3 (S3) achieved R^2 and NSE values of 0.452 and 0.411 for BB dam and 0.490 and 0.473 for SK dam, respectively on the training dataset. In contrast to daily prediction models with XGBoost, R^2 and NSE values were slightly higher on the testing dataset with the values of 0.679 and 0.675 for BB dam and 0.520 and 0.513 for SK dam, respectively. However, MSE and RMSE values were significantly decreased by -69.70% and -44.85% for BB dam and -34.70% and -19.19% for SK dam when testing dataset was accordingly employed. DL-based monthly univariate prediction using LSTM in Scenario 4 (S4) exhibited higher statistical performances in terms of R^2 and NSE values of 0.519 and 0.513 for BB dam and 0.678 and 0.673 for SK dam, respectively. However, these performance metrics considerably decreased to 0.388 and 0.353 for BB dam and 0.434 and 0.407 for SK dam when the testing datasets were investigated. The MSE and RMSE values performed by monthly prediction model with LSTM were significantly decreased by -34.34% and -18.98% for BB dam. In contrast, it showed the substantial increase in MSE and RMSE values by +53.24% and +23.23% for SK dam when testing dataset was accordingly employed. Compared to the individual monthly prediction by LSTM on testing datasets, LSTM-based monthly multivariate prediction in Scenario 6 (S6) could predict better results achieving R^2 and NSE values of 0.526 and 0.397 for BB dam and 0.487 and 0.459 for SK dam, respectively. However, it showed lower R^2 and NSE values compared to those obtained by individual monthly prediction using XGBoost.

407

408

In comparison between daily and monthly prediction models, the results demonstrated that ML- and DL-based prediction models achieved higher statistical metrics in predicting daily reservoir inflow compared to monthly predictions. This is because prediction modeling with ML and DL algorithms can handle and leverage larger datasets available in daily prediction model, enabling them to learn and capture patterns more effectively. Similarly, training larger datasets with LSTM for both daily and monthly univariate and multivariate prediction models mostly outperformed XGBoost. However, slight decrease in statistical metrics is found when dealing with the smaller testing datasets. To improve the robustness and precision of LSTM-based forecasts for both univariate and multivariate predictions, it is recommended to increase the testing dataset size during model validation. Importantly, cross-validation should be conducted to assess model overfitting and ensure its generalizability.

409

410

411

412

413

414

415

416

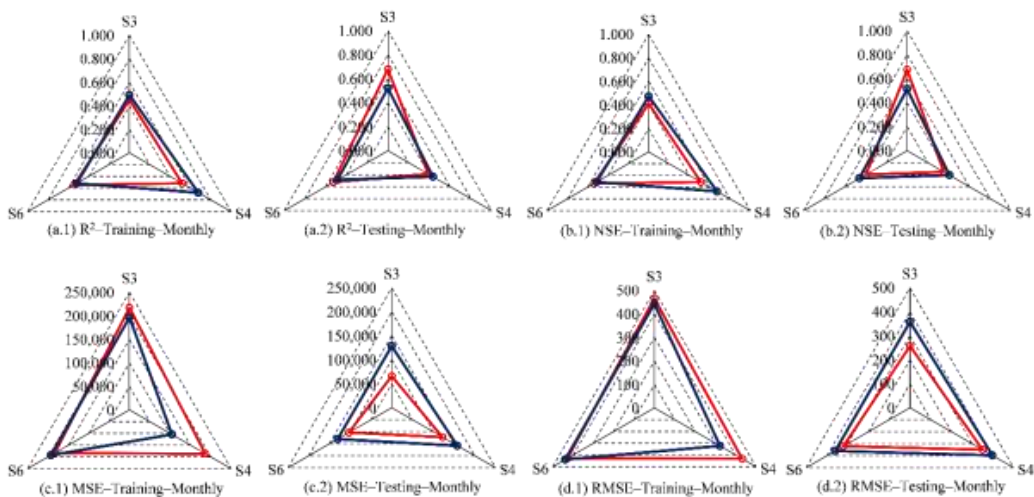


Fig. 8 Radar chart illustrating the performance metrics of all scenarios of 1-month ahead reservoir inflow prediction (Legend: Red–BB, Blue–SK)

417
 418
 419
 420
 421
 422
 423

3.2. Optimal model configuration for univariate and multivariate reservoir inflow prediction models

Based on the optimization criteria of maximizing R^2 and NSE values as optimal prediction model, accordingly the optimal input features, training and testing dataset ratio, and optimal hyperparameter of prediction models were explored. The results of optimal model configuration are summarized in Table 7.

Table 7 Optimal model configuration for reservoir inflow prediction models

| Input Features & Training:Testing Ratio & Hyperparameter | S1: Daily Univariate Model_XGBoost | | S2: Daily Univariate Model_LSTM | | S3: Monthly Univariate Model_XGBoost | | S4: Monthly Univariate Model_LSTM | | S5: Daily Multivariate Model_LSTM | S6: Monthly multivariate Model_LSTM |
|--|------------------------------------|--------|---------------------------------|--------------|--------------------------------------|--------|-----------------------------------|--------------|-----------------------------------|-------------------------------------|
| | BB | SK | BB | SK | BB | SK | BB | SK | BB-SK | BB-SK |
| Past Inflow at Time t | ✓ | ✓ | ✓ | ✓ | ✓ | ✓ | ✓ | ✓ | ✓ | ✓ |
| Avg. Past Inflow at t-3 | ✓ | ✓ | — | — | ✓ | — | ✓ | ✓ | ✓ | ✓ |
| Avg. Past Inflow at t-7 | — | — | ✓ | ✓ | — | ✓ | — | — | — | — |
| Rainfall at Time t | — | — | — | — | ✓ | ✓ | — | — | ✓ | ✓ |
| Humidity at Time t | — | — | — | — | ✓ | — | — | — | ✓ | ✓ |
| Training:Testing Ratio | 80:20 | 80:20 | 70:30 | 70:30 | 80:20 | 70:30 | 60:40 | 60:40 | 70:30 | 60:40 |
| XGBoost: Learning Rate | 0.1 | 0.1 | — | — | 0.001 | 0.001 | — | — | — | — |
| XGBoost: Nrounds | 10,000 | 10,000 | — | — | 10,000 | 10,000 | — | — | — | — |
| XGBoost: Max Depth | 6 | 6 | — | — | 6 | 6 | — | — | — | — |
| LSTM: Learning Rate | — | — | 0.1 | 0.1 | — | — | 0.1 | 0.1 | 0.1 | 0.1 |
| LSTM: No. of Layers | — | — | 2 | 2 | — | — | 2 | 2 | 2 | 2 |
| LSTM: No. of Units | — | — | 64 | 64 | — | — | 64 | 64 | 64 | 64 |

424
 425
 426
 427
 428
 429
 430
 431
 432
 433
 434
 435
 436

It is emphasized that information on past reservoir inflow including the previous time step and its moving average was observed to be a significant predictor to predict future inflow for all prediction scenarios. For daily and monthly multivariate predictions by LSTM, rainfall and humidity data was incorporated as input features which demonstrated a substantial impact on predictive performances. Since XGBoost can work effectively with smaller datasets compared to LSTM for both univariate and multivariate prediction models, it is crucial to select key predictors that are highly correlated with reservoir inflow for the model development. Conversely, LSTM is specifically designed for larger sequential datasets, a broad range of potential input features can be included in the prediction models. Moreover, altering optimal training and testing ratios by increasing the testing datasets into 70:30 and 60:40 can significantly enhance the predictive performances of optimal LSTM-based prediction models. However, handling the larger datasets require more computational resource to capture relevant data features making LSTM-based prediction models computationally expensive than XGBoost. Furthermore, multivariate prediction models generally consume more computational resources than univariate prediction models.



437 It is revealed from the model configuration experiment that learning rate of 0.1 and 0.001 significantly
438 impacts stability and convergence of both XGBoost and LSTM algorithms during model training. The number of
439 boosting rounds (nrounds) of 10,000 in all scenarios of XGBoost-based prediction models can improve the statistical
440 performance metrics substantially. However, overfitting risk due to increased number of boosting rounds should be
441 carefully investigated through model validation. In this study, to control complexity of individual tree and capture
442 complex data pattern from deeper trees, maximum depth was set to 6 for all scenarios of univariate prediction. For the
443 LSTM-based prediction models, learning rate of 0.1 of both univariate and multivariate prediction models is a
444 significant hyperparameter in achieving model stability and convergence. Number of layers was set to 2 across all
445 prediction scenarios to identify model complexity. Furthermore, the optimal number of LSTM units was observed to
446 be 64 across all scenarios exhibiting increased predictive performances.
447

448 **3.3. Evaluation of Percentage Error of Low, Average and High Reservoir Inflow Prediction**

449 The percentage error of low, average and high reservoir inflow prediction, was computed to diagnose the
450 predictability of ML- and DL-based prediction models as summarized the results in Table 8. It is revealed that the
451 daily minimum and average reservoir inflows performed by XGBoost univariate model (S1) on the training and testing
452 datasets were very close to the observed values. On the training datasets, a small discrepancy of daily minimum and
453 average reservoir inflows was +0.17 MCM and -0.81 MCM (-4.62% error), respectively for BB dam and +3.03 MCM
454 and -0.62 MCM or -3.58%, respectively for SK dam. Similarly, it showed small discrepancy of daily minimum and
455 average reservoir inflows on the testing datasets was +0.17 MCM and +0.03 MCM (+0.27% error), respectively for
456 BB dam and +3.03 MCM and -0.34 MCM or -2.38%, respectively for SK dam. Importantly, this analysis exhibited
457 a consistent overprediction of minimum reservoir inflows for these two dams on both training and testing datasets. In
458 contrast, larger percentage error in underprediction of maximum reservoir inflows on both training and testing datasets
459 were observed ranging -36.73% and -6.93%, respectively for BB dam and -33.77% and -46.78%, respectively for
460 SK dam. While, the small percentage error of average reservoir inflows predicted by XGBoost univariate model varied
461 positively and negatively relative to observed values indicating both under- and overprediction.
462

463 Similar to XGBoost, the predictive results performed using LSTM (S2) for daily univariate prediction showed
464 the small discrepancy in minimum and average reservoir inflows of BB and SK dams. However, bigger discrepancy
465 was observed in maximum inflow prediction for these two dams. On the training datasets, discrepancy error in
466 minimum, average, and maximum reservoir inflows were +0.27 MCM, +0.26 MCM (+1.74% error), and -9.87 MCM
467 (-3.17% error), respectively, for BB dam, and +1.62 MCM, -0.05 MCM (-0.32% error), and -11.71 MCM (-5.46%),
468 respectively, for SK dam. On testing datasets, LSTM model exhibited small discrepancy error in minimum, average,
469 and maximum reservoir inflows by +0.27 MCM, +0.65 MCM (+6.00% error), and +18.05 MCM (+9.63% error),
470 respectively, for BB dam, and +1.14 MCM, +0.04 MCM (+0.30% error), and -11.14 MCM (-5.09%), respectively,
for SK dam.

471 For the daily multivariate prediction model using LSTM (S5), the discrepancy of minimum, average, and
472 maximum reservoir inflows of two dams were definitely close to those obtained from univariate prediction models
473 using two algorithms; XGBoost and LSTM. The daily minimum reservoir inflows performed by multivariate
474 prediction model for BB and SK dams were +0.20 MCM and +2.65 MCM, respectively on training datasets, and +0.21
475 MCM and +2.65 MCM, respectively on testing datasets. These predictive results were slightly overpredicted
476 compared to the minimum observed values. In addition, the daily average inflows for BB and SK dams on the training
477 datasets, were slightly underpredicted by -2.74% and -2.50%, respectively. On the testing datasets, overprediction
478 was observed, with values of +4.37% and +6.48%, respectively. Similar to the univariate models, multivariate
479 prediction models consistently underpredicted maximum reservoir inflows for both BB and SK dams, as obviously
480 found in both training and testing datasets.
481

482 All in all, the LSTM univariate model (S2) exhibited the smallest percentage errors in predicting minimum,
483 average, and maximum reservoir inflows for daily predictions compared to the XGBoost model (S1) and multivariate
484 prediction using LSTM (S5). Among all ML- and DL-based prediction models (S1, S2, and S5) for daily prediction,
485 underprediction of low reservoir inflows and overprediction of high reservoir inflows by both univariate and
486 multivariate prediction models were consistently emerged. However, LSTM-based individual prediction model is
487 recommended for high inflow prediction.
488
489
490
491
492



493

Table 8 Percentage error of low, average and high reservoir inflow prediction

| Model Type | Optimal Prediction Model | | | | | Min. Reservoir Inflow (MCM) | | | Avg. Reservoir Inflow (MCM) | | | Max. Reservoir Inflow (MCM) | | |
|-------------------------------------|--------------------------|-------------------|---------------|-----|----------|-----------------------------|--------|---------------------|-----------------------------|--------|---------------------|-----------------------------|----------|-----------------------|
| | Algorithm | Training: Testing | Learning Rate | Dam | Dataset | Obs. | Pred. | Δ (%) | Obs. | Pred. | Δ (%) | Obs. | Pred. | Δ (%) |
| S1: Daily Univariate Prediction | XGBoost | 80:20 | 0.1 | BB | Training | 0.00 | 0.17 | +0.17 | 17.52 | 16.71 | -0.81 (-4.62) | 311.46 | 197.05 | -114.41 (-36.73) |
| | | | | BB | Testing | 0.00 | 0.17 | +0.17 | 10.99 | 11.02 | +0.03 (+0.27) | 156.57 | 145.71 | -10.86 (-6.94) |
| | XGBoost | 80:20 | 0.1 | SK | Training | 0.00 | 3.03 | +3.03 | 17.32 | 16.70 | -0.62 (-3.58) | 221.87 | 146.95 | -74.92 (-33.77) |
| | | | | SK | Testing | 0.00 | 3.03 | +3.03 | 14.26 | 13.92 | -0.34 (-2.38) | 218.70 | 116.39 | -102.31 (-46.78) |
| S2: Daily Univariate Prediction | LSTM | 70:30 | 0.1 | BB | Training | 0.00 | 0.27 | +0.27 | 14.90 | 15.16 | +0.26 (+1.74) | 311.46 | 301.59 | -9.87 (-3.17) |
| | | | | BB | Testing | 0.00 | 0.27 | +0.27 | 10.83 | 11.48 | +0.65 (+6.00) | 187.34 | 205.39 | +18.05 (+9.63) |
| | LSTM | 70:30 | 0.1 | SK | Training | 0.00 | 1.62 | +1.62 | 15.81 | 15.76 | -0.05 (-0.32) | 214.42 | 202.71 | -11.71 (-5.46) |
| | | | | SK | Testing | 0.00 | 1.14 | +1.14 | 13.25 | 13.29 | +0.04 (+0.30) | 218.70 | 207.56 | -11.14 (-5.09) |
| S3: Monthly Univariate Prediction | XGBoost | 80:20 | 0.001 | BB | Training | 0.00 | 8.05 | +8.05 | 476.49 | 360.10 | -116.39 (-24.43) | 2,990.21 | 1,811.99 | -1,178.22 (-39.40) |
| | | | | BB | Testing | 12.99 | 10.87 | -2.12 (-16.32) | 370.31 | 359.75 | -10.56 (-2.85) | 2,373.51 | 1,740.76 | -632.75 (-26.66) |
| | XGBoost | 70:30 | 0.001 | SK | Training | 61.48 | 78.04 | +16.56 (+26.94) | 543.94 | 479.97 | -63.97 (-11.76) | 3,095.97 | 2,076.67 | 1,019.30 (-32.92) |
| | | | | SK | Testing | 40.30 | 83.60 | +43.30 (+107.44) | 429.62 | 437.75 | +8.123 (+1.89) | 2,026.29 | 1,432.32 | -593.97 (-29.31) |
| S4: Monthly Univariate Prediction | LSTM | 70:30 | 0.1 | BB | Training | 0.00 | 56.53 | +56.53 | 460.61 | 479.25 | +18.64 (+4.05) | 2,877.23 | 2,373.81 | -503.42 (-17.50) |
| | | | | BB | Testing | 9.03 | 116.48 | +107.45 (+1,190) | 336.64 | 410.65 | +74.01 (+21.98) | 1,944.38 | 1,469.24 | -475.14 (-24.44) |
| | LSTM | 70:30 | 0.1 | SK | Training | 46.50 | 110.20 | +63.70 (+136.99) | 486.21 | 495.34 | +9.14 (+1.88) | 3,095.97 | 2,477.07 | -618.90 (-19.99) |
| | | | | SK | Testing | 40.30 | 112.55 | +72.25 (+179.28) | 410.14 | 460.03 | +49.89 (+12.17) | 2,026.29 | 1,845.41 | -180.88 (-8.93) |
| S5: Daily Multivariate Prediction | LSTM | 60:40 | 0.1 | BB | Training | 0.00 | -0.20 | -0.20 | 17.52 | 17.04 | -0.48 (-2.74) | 311.46 | 161.51 | -149.95 (-48.14) |
| | | | | BB | Testing | 0.00 | -0.21 | -0.21 | 10.99 | 11.47 | +0.48 (+4.37) | 156.57 | 151.09 | -5.48 (-3.50) |
| | LSTM | 60:40 | 0.1 | SK | Training | 0.00 | 2.65 | +2.65 | 18.38 | 17.92 | -0.46 (-2.50) | 221.87 | 121.05 | -100.82 (-45.44) |
| | | | | SK | Testing | 0.00 | 2.65 | +2.65 | 14.20 | 15.12 | +0.92 (+6.48) | 218.70 | 118.95 | -99.75 (-45.61) |
| S6: Monthly Multivariate Prediction | LSTM | 70:30 | 0.1 | BB | Training | 0.00 | 17.92 | +17.92 | 510.59 | 551.76 | +41.17 (+8.06) | 2,990.21 | 1,984.74 | 1,005.47 (-33.63) |
| | | | | BB | Testing | 1.57 | 16.09 | +14.52 (+924.84) | 323.19 | 455.97 | +132.78 (+41.08) | 2,373.51 | 1,481.92 | -891.59 (-37.56) |
| | LSTM | 60:40 | 0.1 | SK | Training | 61.48 | 38.49 | -22.99 (-37.39) | 563.63 | 551.53 | -12.097 (-2.15) | 3,095.97 | 2,258.06 | -837.91 (-27.06) |
| | | | | SK | Testing | 40.30 | 54.61 | +14.309 (+35.51) | 428.26 | 485.17 | +56.91 (+13.29) | 2,026.29 | 1,688.66 | -337.631 (-16.66) |

494

495 In view of the crucial role of accurate long-term reservoir inflow predictions in effective reservoir
 496 management planning, this study focuses on developing robust monthly inflow prediction models. Even both
 497 monthly univariate and multivariate prediction models efficiently learned and captured the inflow patterns, exhibiting
 498 similarities to observed values, monthly prediction models (S3, S4, and S6) demonstrated larger deviations from
 499 observed values with higher percentage errors compared to daily predictions (S1, S2, and S5). On the training
 500 datasets of S3, a bigger discrepancy of monthly minimum reservoir inflows was +8.05 MCM and +16.56 MCM for
 501 BB and SK dams, respectively. While, the monthly average and maximum reservoir inflows were -24.43% and
 502 -39.40%, respectively for BB dam and -11.76% and -39.92%, respectively for SK dam. Base on the testing datasets,
 503 the percentage errors particularly in monthly minimum and maximum inflows were found to be underpredicted by
 504 -16.32% for BB dam and overpredicted by +107.44% for SK dam. The maximum reservoir inflows of both BB and
 505 SK dams were underpredicted with the errors of -26.66% and -29.31%, respectively. Analysis of monthly minimum



506 and average inflows for both training and testing datasets of S4 and S6 revealed overprediction primarily for BB and
507 SK dams. Conversely, monthly maximum reservoir inflows were consistently underpredicted, exhibiting larger
508 percentage errors.

509
510 **4. Conclusion**

511 This study demonstrated the ability of ML- and DL- based univariate and multivariate prediction models to
512 predict daily and monthly reservoir inflows of BB and SK dams. Due to a wide range of successful applications of
513 ML and DL algorithms for hydrological prediction, XGBoost, a tree- based ensemble method, and LSTM, a deep
514 neural network, were selected for this study. To support real- time reservoir operation for the BB and SK dams, two
515 short- term prediction scenarios (S1 and S2) of daily univariate models and one scenario (S5) of daily multivariate
516 models were developed. In addition, two long- term prediction scenarios (S3 and S4) of monthly univariate models
517 and one scenario (S6) of monthly multivariate models were developed to support reservoir management planning. For
518 univariate prediction, the inflows of the BB and SK dams were predicted separately using two individual models. In
519 contrast, for multivariate prediction, a single model was developed to simultaneously predict the inflows of both the
520 BB and SK dams facilitating the integrated decision- making processes in the river basin. The results of all prediction
521 scenarios demonstrated that ML- and DL- based prediction models achieved higher statistical metrics evaluated in
522 terms of R^2 , NSE, MSE, and RMSE in predicting daily reservoir inflow compared to monthly predictions. This is
523 because prediction modeling with ML and DL algorithms can handle and leverage larger datasets available in daily
524 prediction model, enabling them to learn and capture patterns more effectively. Based on a number of model
525 configuration experiments, individual XGBoost models mostly outperformed LSTM when tested on the datasets for
526 both daily and monthly univariate predictions. LSTM models consistently outperformed XGBoost when mostly
527 trained on larger datasets for both daily and monthly univariate and multivariate predictions. However, a slight
528 decrease in statistical metrics was apparently observed with smaller testing datasets. To enhance the robustness and
529 precision of LSTM- based forecasts, it is recommended to increase the testing dataset size during model validation
530 and employ cross-validation techniques to check for model overfitting. For input feature selection, the information on
531 past reservoir inflow including the previous time step and its moving average was considered as a significant predictor
532 to predict future inflow for all prediction scenarios. As LSTM can handle large datasets effectively, consequently,
533 rainfall and humidity data were also incorporated as additional input features indicating a substantial impact on
534 improved predictive performance. Ability to predict low, average, and high reservoir inflow by ML- and DL- based
535 prediction models were also assessed. Overall, LSTM- based univariate model distinctively exhibited the smallest
536 percentage errors in predicting minimum, average, and maximum reservoir inflows for daily and monthly predictions
537 compared to the XGBoost model and multivariate prediction using LSTM. Consequently, LSTM- based individual
538 daily and monthly prediction models are recommended for predicting low and high values of reservoir inflow during
539 critical events. In addition, monthly prediction models demonstrated larger discrepancy from observed values with
540 higher percentage errors compared to daily predictions. Among all ML- and DL- based prediction models for daily
541 and monthly predictions, underprediction of low reservoir inflows and overprediction of high reservoir inflows by
542 both univariate and multivariate prediction models were consistently existed. Therefore, extracting specific and
543 informative insights from the results of each prediction model and forecasting horizon can significantly enhance
544 decision- making support for both real- time reservoir operation and long- term reservoir management planning.

545
546 **Code and data availability statement**

547 The data and code are available upon request from the corresponding author.

548

549 **Interactive computing environment**

550 An R- based environment utilizing the Dplyr, ggplot2, imputeTS, Matrix, Metrics, RcppRoll, and Xgboost
551 libraries was used for developing XGBoost- based prediction models. A custom Python- based environment
552 leveraging RNN, Reticulate, Modeler, Keras, and other relevant Python libraries was employed for the development
553 of LSTM- based prediction models.

554

555 **Author contribution**

556 All authors contributed to the study conception and design. Material preparation, data collection and
557 analysis were performed by Areeya Rittima, Jidapa Kraisangka, and Pheeranat Dornpunya. The first draft of the
558 manuscript was written and reviewed by Areeya Rittima, Jidapa Kraisangka, Pheeranat Dornpunya and all authors
559 commented on previous versions of the manuscript. All authors read and approved the final manuscript.

560

561



562 **Completing interests**

563 The authors declare that they have no known competing financial interests or personal relationships that
564 could have appeared to influence the work reported in this paper.

565

566

567 The authors declare that they have no conflict of interest.

568

569 **Acknowledgements**

570 This research was funded by the Office of the National Research Council of Thailand (NRCT). The authors
571 are grateful to the Royal Irrigation Department (RID), Electricity Generating Authority of Thailand (EGAT) for
572 providing research data.

573

574 **Financial support**

575 This work was financially supported by the National Research Council of Thailand (NRCT), grant numbers
576 SIP6230022. A Rittima received research support from NRCT in 2021.

577

578 **Review statement**

579 This study demonstrated the predictability of Machine Learning (ML)– and Deep Learning (DL)–based
580 univariate and multivariate predictions of reservoir inflows of Bhumibol (BB) and Sirikit (SK), two major dams in the
581 Chao Phraya River Basin. XGBoost, tree-based ensemble–, and LSTM, deep neural network–based algorithms were
582 selected for development of daily and monthly prediction models. Input features selection and configuration design
583 of two different types of daily and monthly reservoir inflow prediction models; (1) univariate prediction with XGBoost
584 and LSTM algorithms and (2) multivariate prediction with LSTM algorithm, were definitely highlighted. In the last
585 step, predictability of predicting low and high reservoir inflow values of these models were accordingly explored to
586 assess their statistical performances.

587

588 **References**

589 Ahmed, A.N., Yafouz, A., Birima, A.H., Kisi, O., Huang, Y.F., Sherif, M., Sefelnasr, A., and El-Shafie, A.: Water level
590 prediction using various machine learning algorithms: a case study of Durian Tunggal river, Malaysia, Eng.
591 Appl. Comput. Fluid Mech., 16(1), 422–440, <https://doi.org/10.1080/19942060.2021.2019128>, 2021.
592 Al-Aqeeli, Y.H., Almohseen, K.A., Lee, T.S., and Aziz, S.A.: Modelling monthly operation policy for the Mosul Dam,
593 northern Iraq, J. Hydrol., 5(2), 179–193, 2015.
594 Almubaidin, M.A.A., Latif, S.D., Balan, K., Ahmed, A.N., and El-Shafie, A.: Enhancing sediment transport
595 predictions through machine learning–based multi–scenario regression models, Results in Engineering, 20,
596 101585, <https://doi.org/10.1016/j.rineng.2023.101585>, 2023.
597 Apaydin, H., and Sibtain, M.: A multivariate streamflow forecasting model by integrating improved complete
598 ensemble empirical mode decomposition with additive noise, sample entropy, Gini index and sequence–to–
599 sequence approaches, J. Hydrol., 603, Part A, December 2021, 126831, 2021.
600 Aquil, M.A.I., and Ishak, W.H.W.: Comparison of machine learning models in forecasting reservoir water level. J.
601 Adv. Res. Appl. Sci. Eng. Technol., 31(3), 137–144, <https://doi.org/10.37934/araset.31.3.137144>, 2023.
602 Brownlee, J.: XGBoost with python gradient boosted trees with XGBoost and scikit–learn: machine learning mastery,
603 Australia, 1–115, 2018.
604 Chen, T., and Guestrin, C.: XGBoost: a scalable tree boosting system, University of Washington,
605 <http://dx.doi.org/10.1145/2939672.2939785>, 2016.
606 Chen, W., Xie, X., Wang, J., Pradhan, B., Hong, H., Bui, D.T., Duan, Z., and Ma, J.: A comparative study of logistic
607 model tree, random forest, and classification and regression tree models for spatial prediction of landslide
608 susceptibility, Catena., 151, 147–160, 2017.
609 China National Standardization Management Committee.: GB/T22482-2008 Standard for Hydrological Information
610 and Hydrological Forecasting, China (2008), 2008.
611 Coulibaly, P., Anctil, F., and Bobée, B.: Multivariate reservoir inflow forecasting using temporal neural networks, J.
612 Hydrol. Eng., 6(5), [https://doi.org/10.1061/\(ASCE\)1084-0699\(2001\)6.5\(367\)](https://doi.org/10.1061/(ASCE)1084-0699(2001)6.5(367)), 2001.
613 Dtissibe, F.Y., Abba Ari, A.A., Abboubakar, H., Njoya, A.N., Mohamadou, A., and Thiare, O.: A comparative study
614 of machine learning and deep learning methods for flood forecasting in the Far–North region, Cameroon,
615 Scientific African., 23, March 2024, e02053, 2024.



616 Fan, M., Liu, S., and Lu, D.: Advancing subseasonal reservoir inflow forecasts using an explainable machine
617 learning method, *J. Hydrol. Reg. Stud.*, 50(2023), 101584, <https://doi.org/10.1016/j.ejrh.2023.101584>,
618 2023.

619 Firat, M., and Güngör, M.: Hydrological time-series modelling using an adaptive neuro-fuzzy inference system,
620 *Hydrol. Process.*, 22, 2122–2132, 2008.

621 Haghabi, A.M., Nasrolahi, A.H., and Parsaei, A.: Water quality prediction using machine learning methods, *Water*
622 *Qual. Res. J.*, 53(1), 3–13, <https://doi.org/10.2166/wqrj.2018.025>, 2018.

623 Hameed, M.M., AlOmar, M.K., Abdulrahman Al-Saadi, A.A., and AlSaadi, M.A.: Inflow forecasting using
624 regularized extreme learning machine: Haditha reservoir chosen as case study, *Stoch. Environ. Res. Risk*
625 *Assess.*, 36, 4201–4221, <https://doi.org/10.1007/s00477-022-02254-7>, 2022.

626 Herbert, Z.C., Asghar, Z., and Oroza, C.A.: Long-term reservoir inflow forecasts: enhanced water supply and inflow
627 volume accuracy using deep learning, *J. Hydrol.*, 601(2021), 126676,
628 <https://doi.org/10.1016/j.jhydrol.2021.126676>, 2021.

629 Hochreiter, S., and Schmidhuber, J.: Long short-term memory, *Neural Computation*, 9(8), 1735–1780,
630 <https://doi.org/10.1162/neco.1997.9.8.1735>, 1997.

631 Huang, I., Chang, M., and Lin, G.: An optimal integration of multiple machine learning techniques to real-time
632 reservoir inflow forecasting, *Stoch. Environ. Res. Risk Assess.*, 36, 1541–1561,
633 <https://doi.org/10.1007/s00477-021-02085-y>, 2022.

634 Ibrahim, K.S.M.H., Huang, Y.F., Ahmed, A.N., Koo, C.H., and El-Shafie, A.: Forecasting multi-step-ahead
635 reservoir monthly and daily inflow using machine learning models based on different scenarios, *Appl.*
636 *Intell.*, 53, 10893–10916 (2023), <https://doi.org/10.1007/s10489-022-04029-7>, 2023.

637 Jan, S., Khan, U., Khalil, A., Khan, A.A., Jan, H.A., and Ullah, I.: Use of machine learning techniques in predicting
638 inflow in Tarbela reservoir of Upper Indus Basin, *J. Agric. Meteorol.*, 26(4), 501–504,
639 <https://doi.org/10.54386/jam.v26i4.2676>, 2024.

640 Kawade, V., Kote, H., Gangaji, V., and Kote, A.S.: Univariate time series prediction of reservoir inflow using
641 artificial neural network, *Int. J. Res. Eng. Technol.*, 6(6), 1783–1785, 2019.

642 Khorram, S., and Jehbez, N.: A hybrid CNN–LSTM approach for monthly reservoir inflow forecasting, *Water Resour.*
643 *Manag.*, 37, 4097–4121, <https://doi.org/10.1007/s11269-023-03541-w>, 2023.

644 Khosravi, K., Golkarian, A., Omidvar, E., Hatamiakouieh, J., and Shirali, M.: Snow water equivalent prediction in
645 a mountainous area using hybrid bagging machine learning approaches, *Research Article–Hydrology.*, 71,
646 1015–1031, 2023.

647 Kisi, O., Azamathulla, H.M., Cevat, F., Kulls, C., Kuhdaragh, M., and Fuladipanah, M.: Enhancing river flow
648 predictions: comparative analysis of machine learning approaches in modeling stage–discharge relationship,
649 *RINENG*, 22(2024), 102017, <https://doi.org/10.1016/j.rineng.2024.102017>, 2024.

650 Latif, S.D., and Ahmed, A.N.: Streamflow prediction utilizing deep learning and machine learning algorithms for
651 sustainable water supply management, *Water Resour. Manag.*, 37(8), 3227–3241, 2023.

652 Latif, S.D., and Ahmed, A.N.: Ensuring a generalizable machine learning model for forecasting reservoir inflow in
653 Kurdistan region of Iraq and Australia, *Environment, Development and Sustainability*,
654 <https://doi.org/10.1007/s10668-023-03885-8>, 2024.

655 Luo, B., Fang, Y., Wang, H., and Zang, D.: Reservoir inflow prediction using a hybrid model based on deep learning,
656 *IOP Conf. Series: Materials Science and Engineering* 715 (2020) 012044, <https://doi.org/10.1088/1757-899X/715/1/012044>, 2020.

657 Ngamsanroaj, Y., and Tamee, K.: Improved model using estimate error for daily reservoir inflow forecasting, *ECTI*
658 *Trans. Comput. Inf. Technol.*, 13(2), 170–177, 2019.

659 Osman, A., Afan, H.A., Allawi, M.F., Jaafar, O., Noureldin, A., Hamzah, F.M., Ahmed, A.N., and El-shafie, A.:
660 Adaptive fast orthogonal search (FOS) algorithm for forecasting streamflow, *J. Hydrol.*, 586 (February),
661 124896, <https://doi.org/10.1016/j.jhydrol.2020.124896>, 2020.

662 Pini, M., Scalfini, A., Liaqat, M.U., Ranzi, R., Serina, I., and Mehmood, T.: Evaluation of machine learning techniques
663 for inflow prediction in Lake Como, Italy, *Procedia Computer Science*, 176(2020), 918–927, 2020.

664 Pradeepakumari, B., and Srinivasu, K.: An implementation of artificial neural reservoir computing technique for
665 inflow forecasting of Nagarjuna Sagar dam, *Int. J. Eng. Adv. Technol.*, 8(1), 2277–3878, 2019.

666 Rajesh, M., Anishka, S., Viksit, P.S., and Arohi, S.: Improving short-range reservoir inflow forecasts with machine
667 learning model combination, *Water Resour. Manag.*, 37, 75–90, <https://doi.org/10.1007/s11269-022-03356-1>, 2023.

668 669



670 Rajesh, M., Indranil, P., and Rehana, S.: Reservoir inflow forecasting based on gradient boosting regressor model –a
671 case study of Bhadra Reservoir, India. 18th Annu. Meet. Asia Oceania Geosci. Soc., 64–66,
672 https://doi.org/10.1142/9789811260100_0022, 2022.

673 Ridwan, W.M., Sapitang, M., Aziz, A., Kushiar, K.F., Ahmed, A.N., and El-Shafie, A.: Rainfall forecasting model
674 using machine learning methods: case study Terengganu, Malaysia, *Ain Shams Eng. J.*, 12(2021), 1651–
675 1663, <https://doi.org/10.1016/j.asej.2020.09.011>, 2021.

676 Sapitang, M., Ridwan, W.M., Kushiar, K.F., Ahmed, A.N., and El-Shafie, A.: Machine learning application in
677 reservoir water level forecasting for sustainable hydropower generation strategy, *Sustainability*, 12(15), 6121,
678 <https://doi.org/10.3390/su12156121>, 2020.

679 Shams, M.Y., Elshewey, A.M., El Sayed, M., El kenawy, Ibrahim, A., Talaat, F.M., and Tarek, Z.: Water quality
680 prediction using machine learning models based on grid search method, *Multimed. Tools Appl.*, 83, 35307–
681 35334, <https://doi.org/10.1007/s11042-023-16737-4>, 2024.

682 Soncin, L., Bertini, C., van Andel, S.J., Ridolfi, E., Napolitano, F., Russo, F., and Ramos Sánchez, C.: Forecasting
683 reservoir inflows with long short-term memory models, *EGU General Assembly 2024*, Vienna, Austria, 14–
684 19 Apr 2024, EGU24–11506, <https://doi.org/10.5194/egusphere-egu24-11506>, 2024.

685 Suprayogi, I., Alfian, Joleha, Nurdin, Bochari, and Azmeri: Development of the inflow prediction model on tropical
686 reservoir using adaptive neuro fuzzy inference system, *International Journal of Civil Engineering and
687 Technology (IJCET)*, 11(4), 171–183, 2020.

688 Valipour, M., Banihabib, M.E., and Behbahani, S.M.R.: Comparison of the ARMA, ARIMA, and the autoregressive
689 artificial neural network models in forecasting the monthly inflow of Dez dam reservoir, *J. Hydrol.*,
690 476(2013), 433–441, 2013.

691 Zakaria, M.N.A., Ahmed, A.N., Malek, M.A., Birima, A.H., Khan, M.M.H., Sherif, M., and Elshafie, A.: Exploring
692 machine learning algorithms for accurate water level forecasting in Muda river, Malaysia, *Heliyon* 9(2023),
693 e17689, <https://doi.org/10.1016/j.heliyon.2023.e17689>, 2023.

694 Zhang, F., li, W., Zhang, Y., and Feng, F.: Data driven feature selection for machine learning algorithms in computer
695 vision, *IEEE Internet Things J.*, 5(6), 4262–4272, 2018.

696 Zhang, W., Wang, H., Lin, Y., Jin, J., Liu, W., and An, X.: Reservoir inflow predicting model based on machine learning
697 algorithm via multi-model fusion: A case study of Jinshuitan river basin, *IET Cyber-Syst. Robot.*, 3(3), 265–
698 277. <https://doi.org/10.1049/csy2.12015>, 2021.